Journal of Biosafety and Biosecurity 6 (2024) 157–169

Contents lists available at ScienceDirect

Journal of Biosafety and Biosecurity

journal homepage: www.keaipublishing.com/en/journals/journal-of-biosafety-and-biosecurity/

Research Article

Structure-based discovery of *F. religiosa* phytochemicals as potential inhibitors against Monkeypox (mpox) viral protein

Ranjan K. Mohapatra [a,*,1], Ahmed Mahal [b,1], Pranab K. Mohapatra [c], Ashish K. Sarangi [d,1], Snehasish Mishra [e], Meshari A. Alsuwat [f], Nada N. Alshehri [g], Sozan M. Abdelkhalig [h], Mohammed Garout [i], Mohammed Aljeldah [j], Ahmad A. Alshehri [k], Ahmed Saif [l], Mohammed Abdulrahman Alshahrani [k], Ali S. Alqahtani [l], Yahya A. Almutawif [m], Hamza M.A. Eid [m], Faisal M Albaqami [n], Mohnad Abdalla [o,*], Ali A. Rabaan [p,q,r,*]

[a] Department of Chemistry, Government College of Engineering, Keonjhar 758002, Odisha, India
[b] Department of Medical Biochemical Analysis, College of Health Technology, Cihan University – Erbil, Erbil, Kurdistan Region, Iraq
[c] Department of Chemistry, CV Raman Global University, Bhubaneswar, Odisha, India
[d] Department of Chemistry, School of Applied Sciences, Centurion University of Technology and Management, Balangir, Odisha, India
[e] School of Biotechnology, Campus-11, KIIT Deemed-to-be-University, Bhubaneswar 751 024, Odisha, India
[f] Clinical Laboratory Sciences Department, College of Applied Medical Sciences, Taif University, Al-Taif 21974, Saudi Arabia
[g] Internal Medicine Department, King Khalid University Medical City, College of Medicine, Abha 61481, Saudi Arabia
[h] Department of Basic Medical Sciences, College of Medicine, AlMaarefa University, Riyadh, Saudi Arabia
[i] Department of Community Medicine and Health Care for Pilgrims, Faculty of Medicine, Umm Al-Qura University, Makkah 21955, Saudi Arabia
[j] Department of Clinical Laboratory Sciences, College of Applied Medical Sciences, University of Hafr Al Batin, Hafr Al Batin 39831, Saudi Arabia
[k] Department of Clinical Laboratory Sciences, Faculty of Applied Medical Sciences, Najran University, Najran 61441, Saudi Arabia
[l] Department of Medical Laboratory Sciences, Faculty of Applied Medical Sciences, King Khalid University, Abha 61481, Saudi Arabia
[m] Department of Medical Laboratories Technology, College of Applied Medical Sciences, Taibah University, Madinah 41411, Saudi Arabia
[n] Biology Department, College of Science, Islamic University of Madinah, Madinah 42351, Saudi Arabia
[o] Pediatric Research Institute, Children's Hospital Affiliated to Shandong University, Jinan, Shandong 250022, China
[p] Molecular Diagnostic Laboratory, Johns Hopkins Aramco Healthcare, Dhahran 31311, Saudi Arabia
[q] College of Medicine, Alfaisal University, Riyadh 11533, Saudi Arabia
[r] Department of Public Health and Nutrition, The University of Haripur, Haripur 22610, Pakistan

ARTICLE INFO

Article history:
Received 18 February 2024
Received in revised form 20 May 2024
Accepted 31 May 2024

Keywords:
Monkeypox
Mpox
Phytochemical
Molecular docking
MD simulation
ADMET
QSAR

ABSTRACT

Outbreaks of Monkeypox (mpox) in over 100 non-endemic countries in 2022 represented a serious global health concern. Once a neglected disease, mpox has become a global public health issue. A42R profilin-like protein from mpox (PDB ID: 4QWO) represents a potential new lead for drug development and may interact with various synthetic and natural compounds. In this report, the interaction of A42R profilin-like protein with six phytochemicals found in the medicinal plant *Ficus religiosa* (abundant in India) was examined. Based on the predicted and compared protein–ligand binding energies, biological properties, IC_{50} values and toxicity, two compounds, kaempferol (C-1) and piperine (C-4), were selected. ADMET characteristics and quantitative structure–activity relationship (QSAR) of these two compounds were determined, and molecular dynamics (MD) simulations were performed. *In silico* examination of the kaempferol (C-1) and piperine (C-4) interactions with A42R profilin-like protein gave best-pose ligand-binding energies of –6.98 and –5.57 kcal/mol, respectively. The predicted IC_{50} of C-1 was 7.63 μM and 82 μM for C-4. Toxicity data indicated that kaempferol and piperine are non-mutagenic, and the QSAR data revealed that piperlongumine (5.92) and piperine (5.25) had higher log P values than the other compounds examined. MD simulations of A42R profilin-like protein in complex with C-1 and C-4 were performed to examine the stability of the ligand–protein interactions. As/C and C-4 showed the highest affinity and activities, they may be suitable lead candidates for developing mpox therapeutic drugs. This study should facilitate discovering and synthesizing innovative therapeutics to address other infectious diseases.

* Corresponding authors.
E-mail addresses: ranjank_mohapatra@yahoo.com (R.K. Mohapatra), mohnadabdalla200@gmail.com (M. Abdalla), arabaan@gmail.com (A.A. Rabaan).
[1] These authors contributed equally to this work and are joint first authors.

https://doi.org/10.1016/j.jobb.2024.05.004

1. Introduction

Monkeypox (mpox) is caused by the mpox virus, a member of the *Poxviridae* family and genus *Orthopoxvirus.*[1] Mpox is a neglected disease primarily endemic to Central and West Africa that emerged in over 100 non-endemic countries in 2022 through community transmission, possibly arising from the endemic countries.[2] Considering its global spread, the WHO declared mpox a public health emergency of international concern on 23 July 2022.[3] West and Central Africa (Congo basin) are the two known mpox clades, the latter being more infectious with high transmissibility.[4] The Central African clade is Type I, and the West African Clade is Type II (with IIa and IIb as two sub-clades). Mpox genomes identified from the 2022 outbreak belong to type II.[5,6]

Infection of the present mpox outbreak was mainly sexually transmitted.[7–9] The virus reached this group via various unclear mechanisms and subsequently circulated among it. Mpox not only circulates among men having sex with men but is becoming a global threat that infects all individuals. Children and immunocompromised are typically at risk and prone to disease severity,[10] with further validation recommended, especially among children. Severe Acute Respiratory Syndrome Coronavirus-2 (SARS-CoV-2) remains a major global concern. Both SARS-CoV-2 and mpox primarily spread and transmit through air-borne droplets. Both may infect simultaneously, which may cause difficulty in the correct diagnosis because their initial symptoms of fever, lymphadenopathy, headache, sore throat and fatigue are similar.[11,12] Furthermore, mpox and STI may also be misdiagnosed because of similar initial symptoms. Nolasco et al. (2022) have also documented the clinical features of a 36-year-old Italian male co-infected with mpox, SARS-CoV-2 and HIV-1.[12] These changing patterns in the spread of mpox are an increasing public health concern that draws attention.[13]

The antiviral tecovirimat is used to treat smallpox and is also recommended for treating mpox.[14] Brincidofovir, cidofovir and vaccinia immunoglobulin intravenous are other valuable antivirals to treat critical cases, e.g., individuals that are pregnant, breastfeeding, elderly and immunocompromised.[14–17] Several neurological complications like headache, myalgia, encephalitis and coma were reported with the recommended vaccines for preventing mpox.[18] Psychiatric complications like anxiety and depression were also reported but with no direct causality. No vaccine afforded 100 % protection, and the efficacy of the available mpox vaccines, JYNNEOSTM and ACAM2000, has been questioned.[19] Moreover, continuous emerging mpox outbreaks in African countries (e.g., Democratic Republic of the Congo) demonstrate that current vaccines and antiviral regimens are inadequate.

Mpox vaccine development is challenging because of numerous reasons. The process of developing a vaccine is costly and time-consuming. Searching for alternatives, such as developing novel drugs, appears prudent. Thus, combined *in silico* studies and *in vitro* assays on drug stability and activity should facilitate the development of effective inhibitors against mpox. Molecular docking is a computational strategy to predict drug binding sites and assist drug repositioning for several diseases, and this strategy plays an important role in designing novel drugs. Identifying a novel chemical scaffold with the potential to inhibit pathogenicity-associated biological targets *in silico* is a promising approach.[20–23]

There is an urgent need to identify and develop new therapeutics against MXPV. Ghate et al. (2024) investigated 5715 phytochemicals from the IMMPAT database as potent inhibitors through molecular docking against six MPXV targets, rifampicin resistance protein (D13L), thymidylate kinase (A48R), DNA ligase (A50R), viral core cysteine proteinase (I7L), palmytilated EEV membrane protein (F13L) and DNA polymerase (E9L).[24] The best-performing phytochemicals were forsythiaside, theasinensin F, ruberythric acid, isocinchophyllamine, theasinensin A and terchebin for inhibiting the activity of A48R, D13L, A50R, I7L, F13L and E9L, respectively. The binding energies of these compounds were far lower than brincidofovir and tecovirimat (standard drugs). A series of natural plant-based biomolecules were investigated in another study to find the most potent inhibitors of MPXV, revealing that dieckol and amentoflavone exhibited high potency with excellent drug-likeness properties with no toxicity.[25] Molecular dynamics (MD) simulations and MM/PBSA techniques confirmed the strong binding affinities of both biomolecules. Six hundred and nine (limonoids, triterpenoids and polyphenols) phytochemicals downloaded from PubChem, ChemSpider and ChEBI databases were virtually screened,[26] revealing that apigenin-7-O-glucuronide and glycyrrhizinic acid inhibit MPXV DNA polymerase activity and represent lead phytochemicals.

Virtual screening was also performed using 1755 FDA-approved small molecule drugs to probe molecular interactions against mpox DdRp.[27] Lumacaftor (–11.7 kcal/mol), betulinic acid (–11.6 kcal/mol), conivaptan (–11.7 kcal/mol), imatinib (–11.2 kcal/mol) and fluspirilene (–11.3 kcal/mol) ranked highest as drug compounds interacting with mpox DdRp.[27] MD simulations (200 ns) with principal component analysis (PCA) were performed to understand the interaction patterns. Sahoo et al. (2023) identified tipranavir, doxorubicin, cefderocol and dolutegravir as potential inhibitor candidates in an *in silico* study using molecular docking and MD simulations to repurpose these four drugs against MPXV.[28]

Patel et al. (2023) qualified Elvitegravir as a potential MPXV inhibitor through an AI-based compound-viral proteins interaction framework.[29] Bansal et al. (2022) screened *Allophylus serratus* phytochemicals against core cysteine proteases of MPXV.[30] N-(2-Allyl carbamoyl-4-chloro-phenyl)-3,4-dimethoxy-benzamide showed the highest binding affinity (–6.7 kcal/mol) among all phytocompounds examined; however, further investigation is required. Gulati et al. (2023) used molecular docking to identify phytochemicals silibinin, oleanolic acid and ursolic acid as having strong binding affinity against three envelope proteins (A26, D13 and H3) of MPXV.[31] The stability of the interaction was further confirmed by MD simulations and MM/PBSA calculations. Patel et al. (2023) screened potent anti-viral phytochemical inhibitors against thymidine kinase (TK) and serine/threonine protein kinase (Ser/Thr kinase), which play a critical role in MPXV replication and virulence, showing that galanthamine had appreciable binding affinity to TK and thalimonine to Ser/Thr kinase.[32] MD simulations showed decent stability of both protein–ligand (P-L) complexes. CHEMBL32926 and CHEMBL4861364, obtained from the ChEMBL database, were identified as two potential inhibitors of a core MPXV cysteine proteinase.[33] In this study, Imran et al. (2023) found respective docking scores of –10.7 and –10.9 kcal/mol and binding free energy ranges of –9.25 to –9.65 kcal/mol and –31.47 to –41.66 kcal/mol for these anti-dengue compounds.[33]

Although the proteome of the mpox virus is essentially unknown, Minasov et al. (2022) reported a 1.52 Å resolution crystal structure of mpox protein A42R for the first time.[34] A42R regulates actin cytoskeleton assembly and has a structure like profilins. The profilin-like A42R (PDB ID: 4QWO; a small actin-binding protein involved in cell development, cytokinesis, membrane trafficking and cell motility) of the Zaire-96-I-16 mpox virus strain was inhibited by designing a targeted drug.[35,36] One of these studies also suggested that the natural biomolecule glycocin F is effective against A42R and has broad-spectrum antiviral potential.[36] A total of 56 bioactive compounds were evaluated recently through molecular docking for their efficacy against a mpox profilin-like protein.[37] This mpox profilin-like protein plays a key role in viral replication and assembly. Curcumin was found to show the stron-

gest binding affinity, followed by gedunin, piperine and coumadin. ADMET assessment showed that these four compounds had no adverse side effects.

Ficus, particularly *F. religiosa*, is commonly found in Asian countries. Chemical analyses revealed that this plant contains many phytoconstituents of pharmaceutical value and biological (antimicrobial, antioxidant, anti-inflammatory, antidiabetic, anticancer, anti-proliferative, antimutagenic, anti-helminthic and immunomodulatory) properties.[38,39] Kaempferol (C-1), methylpiperate (C-2), myricetin (C-3), piperine (C-4), piperlongumine (C-5) and quercetin (C-6) phytochemicals of *F. religiosa* were selected in this study as potential novel therapeutics to treat mpox (Fig. 1). We report the *in silico* binding interaction of these phytochemicals against MPXV through MD simulations. QSAR, pharmacokinetic and drug-likeness predictions are also reported. The study provides information on potential bioactive natural drug candidates that can be used to formulate adjuvant therapy against MPXV.

2. Materials and methods

2.1. Molecular docking and MM/GBSA calculations

Before proceeding with flexible P-L molecular docking, hydrogen atoms were added to the protein and optimized by removing atomic clashes. The ligands were retrieved (in.sdf format) from PubChem. The 3D structures of the ligands were geometrically optimized at pH 7.4 using the MM approach of the open-source YASARA minimization server with the YASARA force field module.[40] The ligands and the protein were saved as.pdbqt files. Attributes like Kollman charges, solvation parameters, polar hydrogens and fragmental volumes were adjusted using the AutoDock tools. The Auto grid engine was used to make a grid box around the binding site of the protein. A 25 × 25 × 25 Å size grid box was prepared with 0.375 Å grid point spacing. Other docking parameters were set at the default values in both programs. The protein and ligands were flexible during the docking procedure. Furthermore, the ligands with the lowest docking score and the best pose binding energy value were further analyzed.

The binding affinities of the six selected phytochemicals were computed by receptor-oriented molecular docking with AutoDock Vina (open-source) software.[41–43] The recently reported 1.52 Å resolution crystal structure of the A42R profilin-like protein of mpox virus (PDB ID: 4QWO) was sourced from the PDB (https://www.rcsb.org/structure/4qwo).[34] The phytochemicals were allowed to interact with this mpox protein, and interactions were visualized using Discovery Studio 3.5. The protein structure facilitated the next level of investigation for leads against mpox.

The prime molecular mechanics generalized born and surface area (MM/GBSA) free energy was computed using the prime energy force field OPLS3e (Schrödinger-Maestro v2020).[44] The free binding energy was calculated using the equation:

$$\Delta G(bind) = E_{complex}(minimized) - E_{ligand}(minimized) + E_{receptor}(minimized) \quad (1)$$

2.2. ADMET and drug-likeness predictions

The ADMET (absorption, distribution, metabolism, excretion and toxicity) pharmacokinetics and the drug-likeness values of the six selected compounds were computed. These were analyzed *in silico* using SwissADME (https://www.swissadme.ch/).[45] The toxicity was assessed using pkCSM (https://biosig.unimelb.edu.au/pkcsm/).[46]

2.3. IC_{50} prediction

The inhibition potential of a ligand to a biological function is measured by half of the maximum inhibitory concentration (i.e., IC_{50}). The IC_{50} values of the test ligands were predicted using AutoDock v4.2.[47] The Lamarkian Genetic Algorithm (LGA) with default *x*, *y* and *z* parameters within 126 Å was chosen, and cluster analysis was performed to obtain the binding energy with IC_{50} values for the docking forms.[48]

2.4. Molecular dynamics simulation

MD simulations were performed to determine the stability of the P-L complexes. MD simulations of A42R profilin-like protein in complex with C1 and C4 were carried out using the Desmond module of the Schrödinger 2020 release. The system was established using the system builder panel of Desmond before proceeding with dynamics simulations. Solvation of the P-L complexes was carried out using a TIP3P water model (12 Å buffer-spaced three-dimensional) cube box and a 12 × 12 × 12 $Å^3$ dimension orthorhombic box. Suitable counter ions were added to maintain

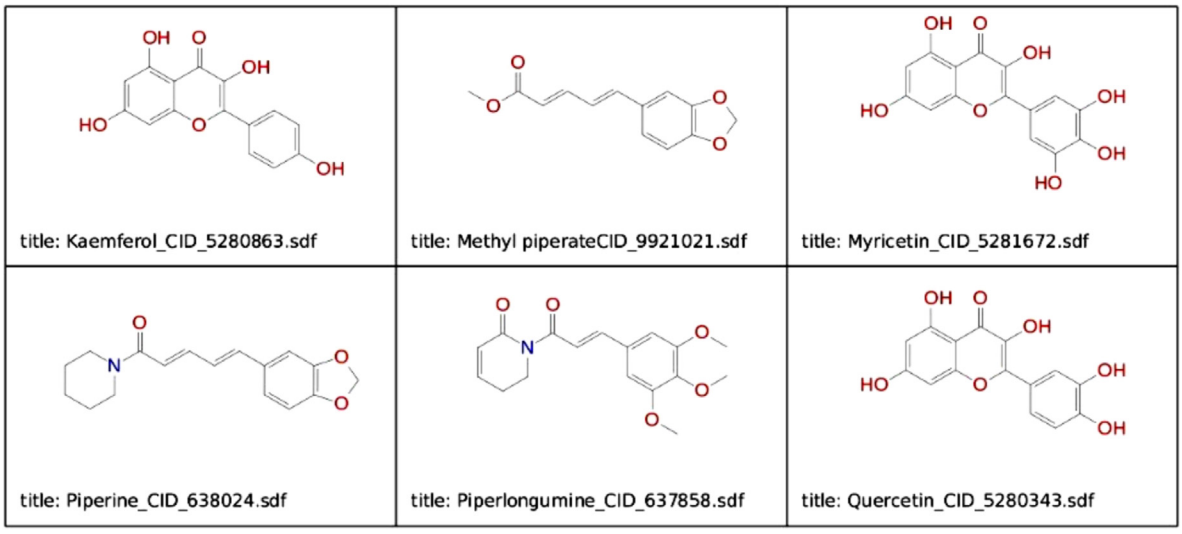

Fig. 1. The structure of the six *F. religiosa*-extracted chemical compounds investigated.

neutrality. 0.15 M NaCl was added to maintain the ionic concentration. The OPLS_2005 force field was used to minimize the energy of the system, applying the steepest descent technique of 10,000 steps with 0–300 K gradual heating in the NVT ensemble. Nose-Hoover chain thermostat and Martyna-Tobias-Klein barostat (relaxing pressure for five ns) techniques were performed before each MD production run. Five hundred nanosecond production runs were carried out under the NPT ensemble using a 12 Å cut-off distance as the system relaxed. The generated 5000 trajectories were saved at 10 ps time-lapses.

3. Results and discussion

3.1. Molecular docking and MM/GBSA binding free energy calculations

We used AutoDock vina for molecular docking to predict the binding interactions between the A42R profilin-like protein and the selected phytochemicals. The six phytochemicals, with GLY A46, GLU A47, PRO A50, LEU A51, ASN A54, ILE A57, LEU A58, LYS A59, PRO A60 and LEU A61 as common amino acid residues, bound to the ligand binding pocket of A42R profilin-like protein. Residues in the active site were predicted using the SCFBio server (https://www.scfbio-iitd.res.in/dock/ActiveSite.jsp). In this study, tecovirimat, a known compound against mpox viral proteins, interacts with the identical active site residues with a binding energy of –8.4 kcal/mol.[35] The binding free energies (best-pose docking scores) were between –5.57 and –6.98 kcal/mol for the six compounds, with kaempferol (C-1) binding yielding the lowest and piperine (C-4) binding yielding the highest values. Tables 1 and 2 detail these interactions. The predicted IC_{50} value for piperine was the lowest (7.63 μM) (Table 1). However, the IC_{50} of all compounds was within the 100 μM permissible concentration.

Mashud et al. (2023) suggested that kaempferol-o-rhamnoside derivatives display anti-viral behavior against mpox.[49] Piperine is a well-known compound often used along with black pepper. Kaempferol (C-1) and piperine (C-4) were selected based on the binding energy results, predicted IC_{50}, ADMET data and literature, and MD simulations were performed. The MM/GBSA calculations reflected the binding free energy of the ligands with the protein. The calculated MM/GBSA ΔG binding free energy for C-1 and C-4 was –33.8234 and –37.3914 kcal/mol, respectively.

3.2. Molecular dynamics simulations

Molecular docking of kaempferol (C-1) and piperine (C-4) with A42R profilin-like protein was determined, yielding the highest binding energy, lowest predicted IC_{50} and best ADMET properties. Thus, C-1 and C-4 were selected for MD simulations. MD simulations (500 ns) were undertaken to characterize the kaempferol-A42R and Piperine-A42R complexes. The RMSD and RMSF values were determined using the MD simulations. The consistency of the complexes was examined by computing the total energy (E), potential energy (E_p), temperature (T), pressure (P) and volume (V).

Table 1
Docking values of the phytochemicals with the A42R profilin-like protein.

Target protein	Compound	Binding energy (kcal/mol)	Predicted IC_{50} values (μM)
A42R profilin-like mpox protein (PDB ID: 4QWO)	C-1: Kaempferol	−5.57	82.56
	C-2: Methylpiperate	−6.07	35.26
	C-3: Myricetin	−5.73	63.10
	C-4: Piperine	−6.98	7.63
	C-5: Piperlongumine	−6.59	14.75
	C-6: Quercetin	−5.64	74.00

3.2.1. Protein RMSD

The constancy of the ligand–protein interactions was confirmed by performing MD simulations of the kaempferol-A42R profilin-like protein and piperine-A42R profilin-like protein complexes, as per earlier reports.[50–53] The RMSD and RMSF values of the MD-simulated complexes were analyzed (Fig. 2). The RMSD of kaempferol and piperine reached a maximum of 2.0 and 2.8 Å, respectively, during the simulations, suggesting the complexes were stable. The RMSD stabilized during the process after initial fluctuations. The kaempferol-A42R profilin-like protein complex was stable during the simulation because the ligand achieved a maximum (i.e., 2 Å) RMSD that gradually decreased and reached an equilibrium < 1.5 Å. Initially fluctuating up to 250 ns with respect to the protein, the RMSD of the ligand reached a maximum of 54 Å at 90 ns and remained stable up to 500 ns, suggesting a displacement and reorientation of the ligand during the simulation. The piperine-A42R profilin-like protein complex adopted a stable conformation as the ligand achieved a maximum (2.8 Å) RMSD that gradually decreased and reached equilibrium at <2.4 Å during the simulation. Initially fluctuating with respect to the protein, the RMSD ligand reached 64 Å at 200 ns and stabilized thereafter, suggesting a displacement and reorientation of the ligand during the simulation. The maximum RMSF was 2.2 Å (kaempferol) and 4.8 Å (piperine) at the binding site (Fig. 2b, d); a deviation of 1–3 Å is acceptable for small globular proteins. The green vertical bars in Fig. 2b, d indicate amino acid residues that interact with the ligand and are involved in ligand binding. The RMSF values for the ligand provide insights into the entropy of the P-L complex.

3.2.2. Ligand properties

The RMSD, the molecular (MolSA), polar (PSA) and solvent accessible (SASA) surface areas, and the radius of gyration (rGyr) ligand properties were computed and analyzed. Initially fluctuating from 0.0–1.5 Å (kaempferol-A42R profilin-like protein), the RMSD of the ligand gradually reached equilibrium at approximately 1.0 Å (Fig. 3). The rGyr value ranged between 3.2 and 3.6 Å and gradually attained equilibrium at 3.4 Å (Fig. 3). The MolSA remained between 244 and 256 $Å^2$, equilibrating at 248 $Å^2$ and remaining nearly constant throughout the simulation. The PSA also reached equilibrium and remained constant, ranging from 220–250 $Å^2$ with equilibrium at 235 $Å^2$. Intramolecular H-bonds ranged between 0 and 1, and SASA ranged between 150 and 450 $Å^2$, fluctuating slightly to 250 ns and gradually approaching equilibrium at ∼250 $Å^2$. In the piperine-A42R profilin-like protein complex, the RMSD of the ligand reached equilibrium at ∼1.0 Å, fluctuating between 0.0 and 1.5 Å (Fig. 4). The rGyr value ranged between 4.4 and 5.0 Å, gradually attaining an equilibrium at 4.6 Å (Fig. 4). The MolSA remained between 288 and 296 $Å^2$, reaching an equilibrium at 292 $Å^2$ and remaining essentially constant throughout. The PSA ranged from 72–84 $Å^2$ with an equilibrium at 78 $Å^2$, and no intramolecular H-bonds were observed. The SASA ranged between 150 and 450 $Å^2$, fluctuating slightly up to 200 ns and gradually approaching an equilibrium at ∼250 $Å^2$. Similar trends were observed for all tested ligand properties with minimal initial fluctuations, gradually reaching equilibrium and remaining constant. The results confirmed the stability of the P-L interaction.

3.2.3. Protein-ligand (P-L) contacts

The P-L contact stability of C1- and C4-A42R profilin-like protein complexes were analyzed (Figs. 5 and 6) following the protocol of Dariya and Nagaraju (2020).[54] Water bridges, ionic, hydrophobic and H-bonding are typical P-L interactions. H-

Table 2
2D and 3D interactions of phytochemicals with the A42R profilin-like protein.

Ligands with	4QWO_Ligand_2D_Interactions	4QWO_Ligand_3D_Interactions
Kaempferol (C-1)	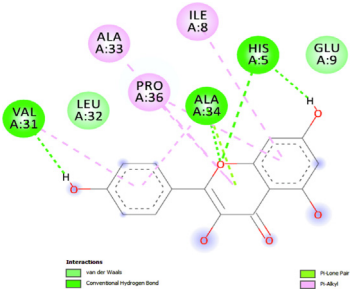	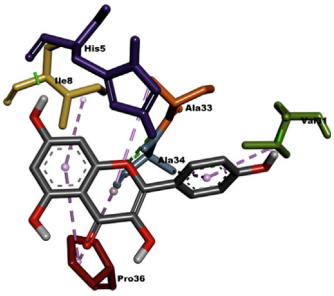
Methylpiperate (C-2)	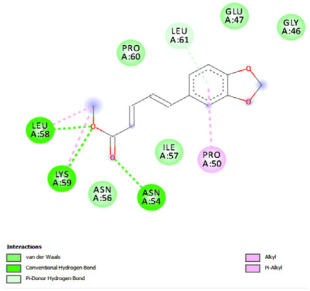	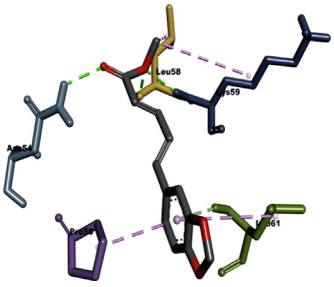
Myricetin (C-3)	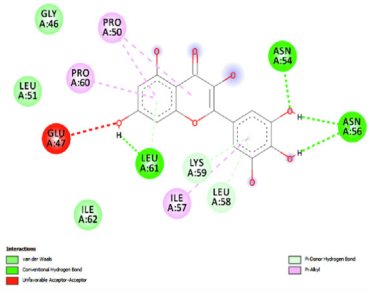	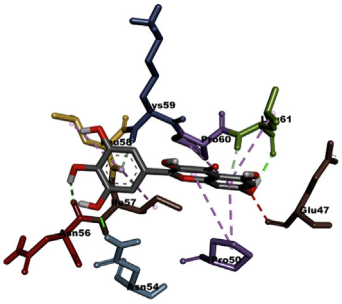
Piperine (C-4)	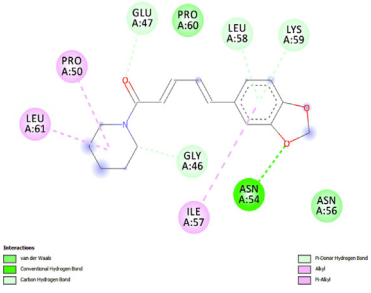	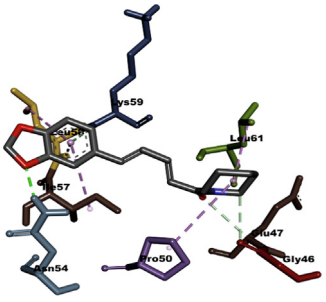
Piperlongumine (C-5)	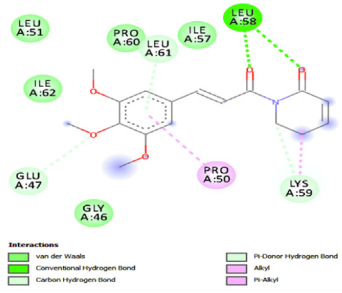	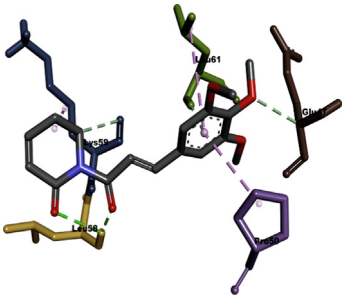

(*continued on next page*)

Table 2 (*continued*)

Ligands with	4QWO_Ligand_2D_Interactions	4QWO_Ligand_3D_Interactions
Quercetin (C-6)	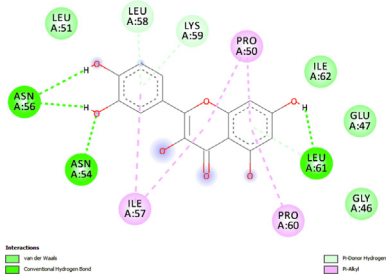	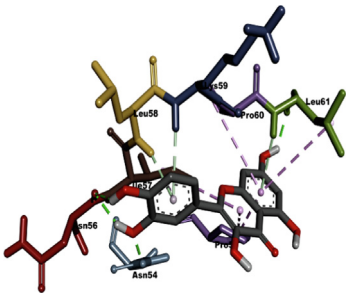

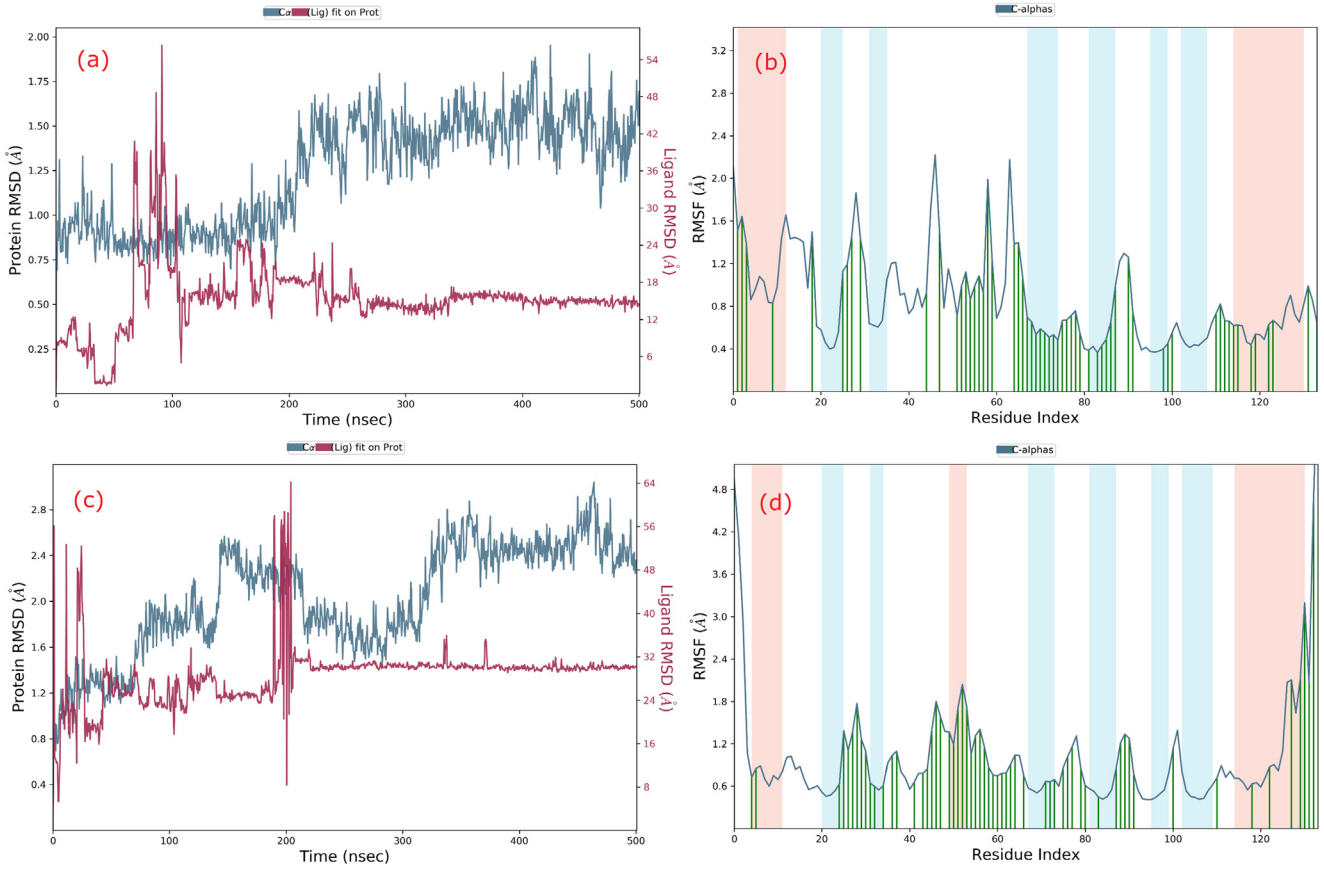

Fig. 2. The protein–ligand RMSD and RMSF trajectories of kaempferol (C-1; a,b) and piperine (C-4; c,d).

bonding is crucial in designing and developing drugs because these non-covalent interactions are critical for ligand binding. The constructed histograms revealed that TYR 25, LYS 26, THR 27, LYS 29, LEU 51, ILE 52, THR 53, ASN 54, HIS 55, ASN 56, ILE 57, LEU 58, VAL 69, TYR 70, THR 71, ASN 72, SER 73, LEU 74, MSE 75, ASP 76, GLU 77, GLU 83, GLY 87, VAL 91, ARG 115, TYR 118, ARG 119, ARG 122 and ASP 123 at the active site of A42R profilin-like protein formed H-bonds with C-1 (kaempferol). TYR 25, LYS 29, ILE 52, HIS 55, LEU 58, ILE 68, VAL 69, TYR 70, VAL 91, ARG 98, PRO 110, ARG 114, ARG 115 and TYR 118 of A42R profilin-like protein mainly formed hydrophobic interactions with C-1 (Fig. 5). TYR 25, LYS 26, LYS 29, GLU 47, LEU 51, ILE 52, THR 53, ASN 54, HIS 55, ASN 56, ILE 57, LEU 58, LYS 59, VAL 69, TYR 70, THR 71, ASN 72, SER 73, MSE 75, ASP 76, GLU 77, ASN 78, THR 79, GLU 83, GLY 87, VAL 91, ARG 98, HIS 100, PRO 110, THR 111, THR 112, ARG 114, ARG 115, TYR 118, ARG 119, ARG 122 and ASP 123 of A42R profilin-like protein interacted with the C-1 ligand via water bridges, whereas LYS 59, TYR 70, THR 71 and ARG 119 formed ionic interactions with the C-1 ligand.

HIS 5, LYS 26, ASN 30, VAL 31, ALA 34, ASN 37, THR 53, ASN 54, ASN 56, LEU 58, LYS 59, LEU 61, GLY 63, GLN 64, TYR 118 and ARG 129 of A42R profilin-like protein formed H-bonds with the C-4 ligand (piperine), whereas TRP 4, HIS 5, TYR 25, VAL 31, LEU 32, PRO 36, ALA 41, ILE 43, PRO 45, ILE 49, PRO 50, LEU 51, ILE 52, HIS 55, ILE 57, PRO 60, LEU 61, ILE 62, PHE 66, TYR 88 and ARG 129 mainly formed hydrophobic interactions with the C-4 ligand (Fig. 6). HIS 5, TYR 25, LYS 26, THR 27, THR 28, LYS 29, ASN 30, VAL 31, LEU 32, ALA 34, ASN 37, ALA 41, ILE 43, ASN 44, GLY 46,

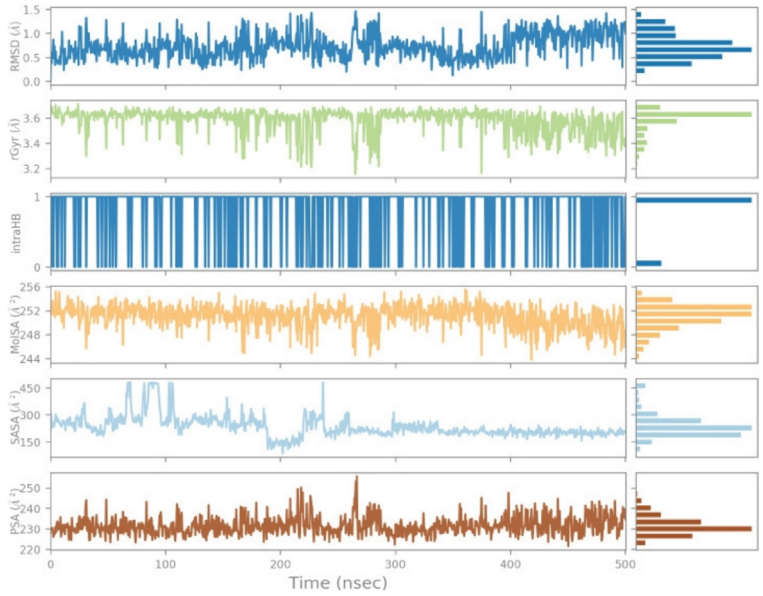

Fig. 3. The ligand property trajectories for the C-1–A42R profilin-like protein complex.

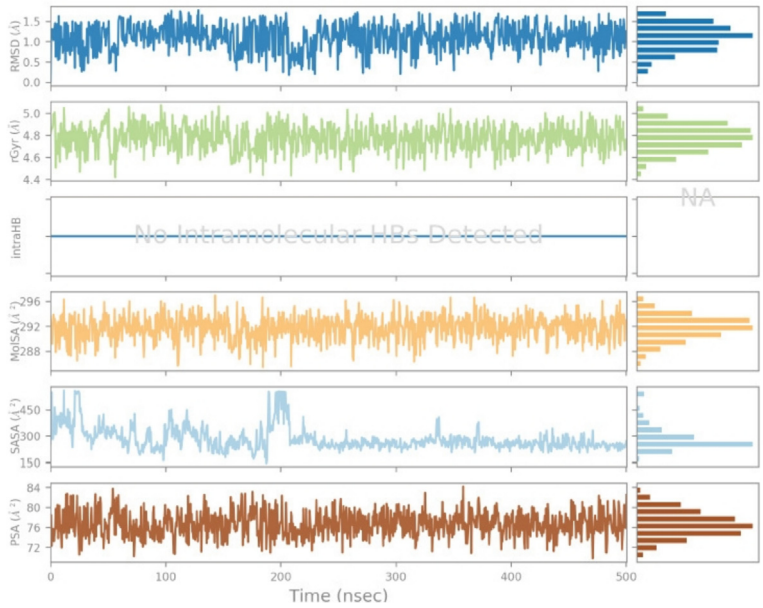

Fig. 4. The ligand property trajectories for the C-4–A42R profilin-like protein complex.

GLU 47, THR 53, ASN 54, HIS 55, ASN 56, LEU 58, LYS 59, LEU 61, GLY 63, GLN 64, ASN 72, SER 73, MSE 75, ASP 76, GLU 77, TYR 80, TYR 88, ALA 89, ARG 129 and ALA 130 interacted with the C-4 ligand through water bridges, whereas the ligand formed no ionic interactions with residues of A42R profilin-like protein (Fig. 6).

The number of contacts for A42R profilin-like protein during the trajectory varied between 0 and 6. The amino acid contribution in trajectory frames was analyzed from the viewpoint of the P-L interaction. Thick bands were observed for the C-1–A42R profilin-like protein complex for HIS 55, ILE 57, LEU 58, VAL 69, TYR 70, THR 71 and ASN 72, and TRP 4, HIS 5 and ALA 34 residues in the C-4–A42R profilin-like protein complex, suggesting more interactions of the above-cited amino acid residues in all possible orientations with the ligands.

3.3. Secondary structure analysis

The α-helical (red) and β-strand (blue) characteristics of A42R profilin-like protein are shown in Fig. 7. The secondary structure region for kaempferol (C-1) covered over 47.07 % of the entire simulation, and for piperine (C-4), the secondary structure region covered over 45.34 %. The upper half of the plot (Fig. 7) reports the SSE distribution by residue index in the protein structure, and the bottom panel summarizes the SSE composition for each trajectory frame during the simulations.

3.4. Physicochemical properties

Physicochemical properties, as a part of the QSAR analysis, predict the characteristics, reactivity and activity of test compounds.

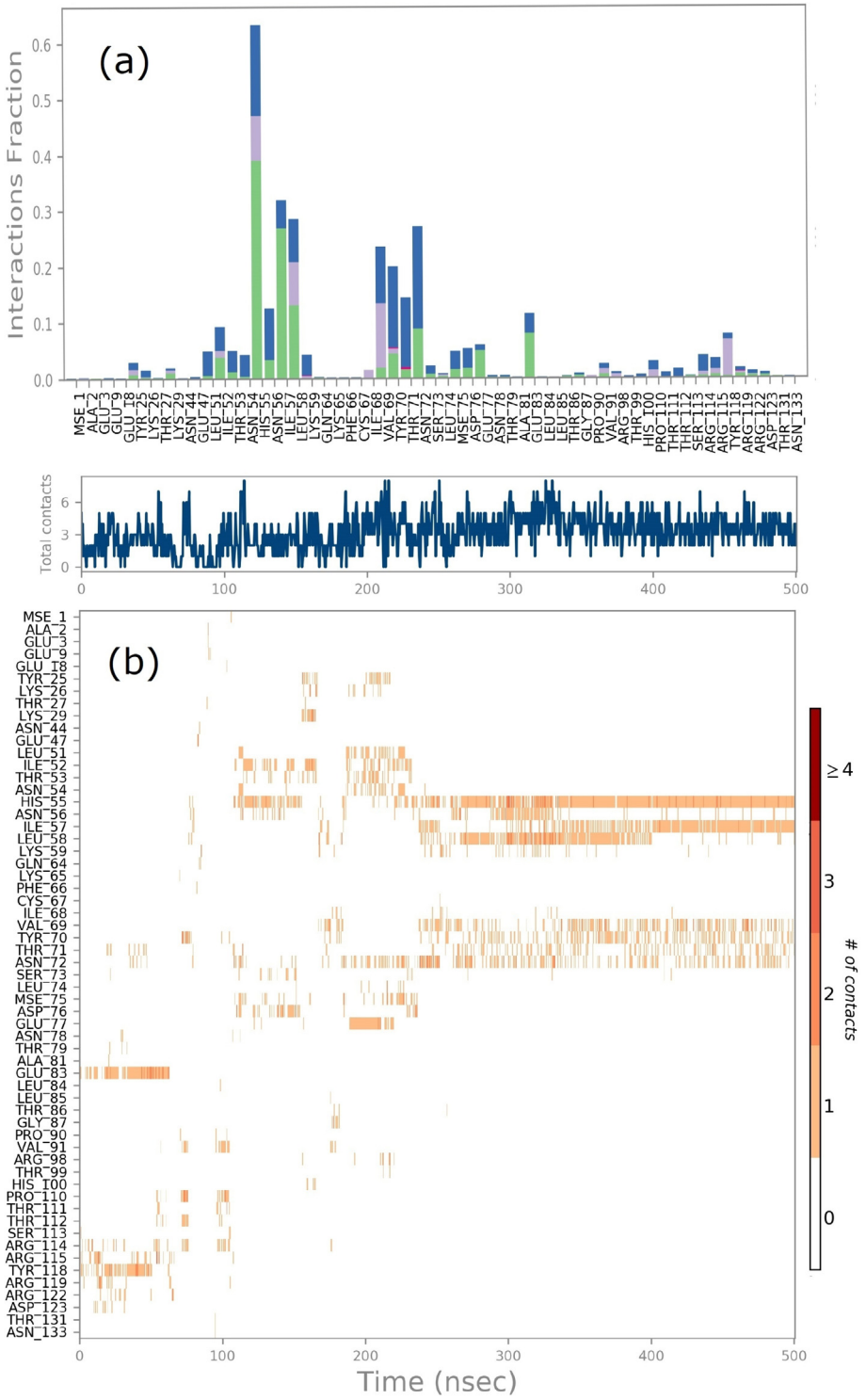

Fig. 5. Protein-ligand contact plots for the C-1–A42R profilin-like protein complex.

We used HyperChem Professional 8.0.3 software for obtaining these properties. The molecular mechanical (MM+) force field and parametric method 3 (PM3, semi-empirical) techniques were used to optimize the structure and Fletcher-Reeves conjugate gradient algorithm so that the energy of ligands was minimized. C-5 returned a higher log P value (5.92) than the other compounds examined. Compounds C1, C2 and C4 also showed appreciable log P values. The measure of log P provides a clear idea of the bioactivity of a test compound, with cell membrane permeation representing the most important function.[55] The calculated volume and molar refractivity of C-5 were significantly higher than other compounds. This result indicated that C-5 had a greater potential to interact with biological targets such as enzymes and receptors because of the greater volume and molar refractivity. Other important physical features of the listed substances were also computed to obtain information about their activity (Table 3).

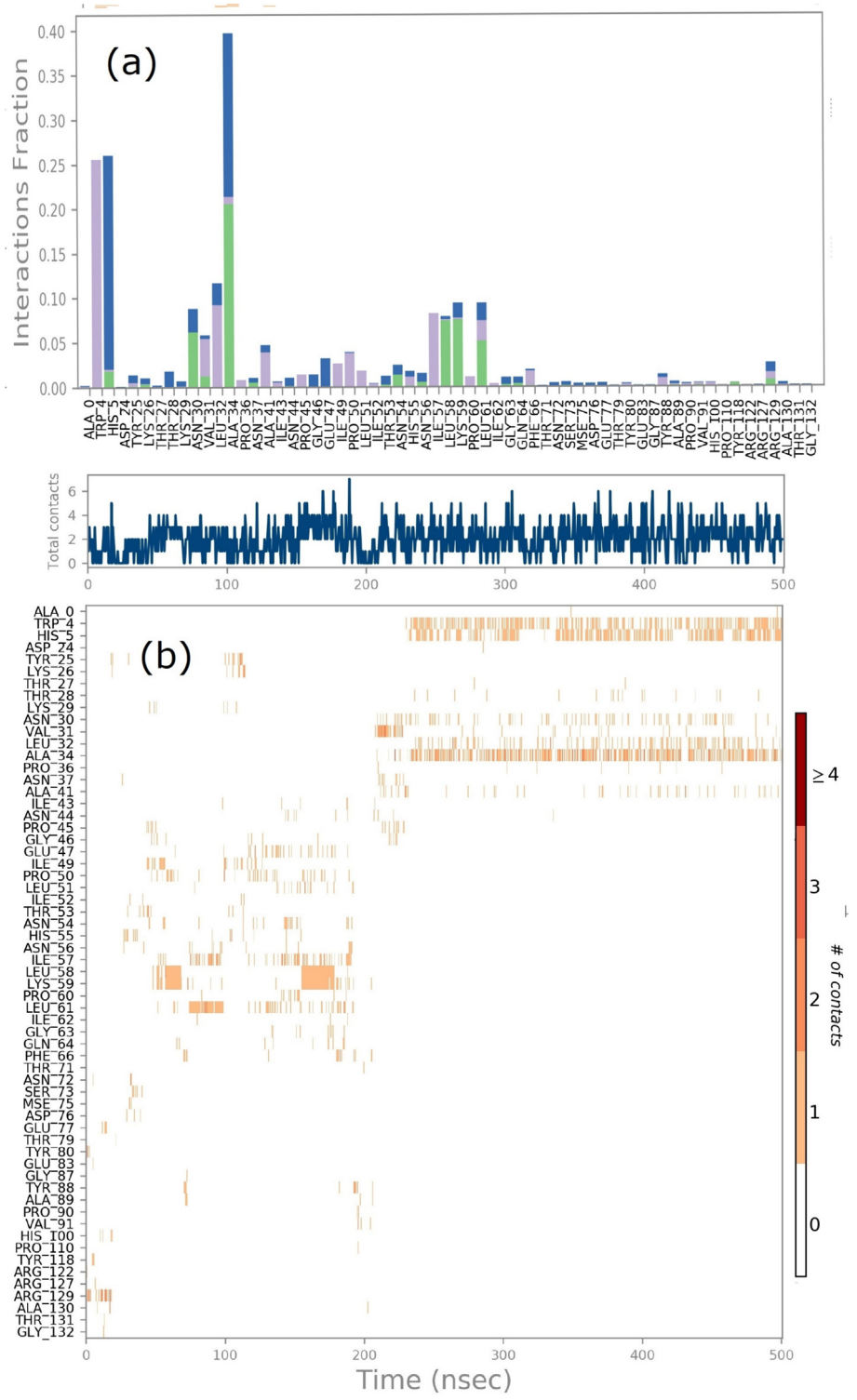

Fig. 6. Protein-ligand contact plots for C-4–A42R profilin-like protein complex.

3.5. Predicting ADMET and drug-likeness properties

Inhibition parameters alone do not qualify a drug as a potential candidate, with ADMET and drug-likeness scores also required for a rational decision on the bio-suitability of a potential drug candidate. The pharmacokinetics, drug-likeness properties and IC_{50} of the test compounds were investigated by *in silico* molecular docking.

ADMET properties (Table 4) were assessed by considering parameters such as gastrointestinal (GI) absorption, skin permeation (log Kp), P glycoprotein (Pgp) inhibition, blood–brain barrier (BBB) and cytochrome (CYP). The predicted values showed that all compounds except myricetin (C-3) had high GI absorption. The generated boiled egg graph (Fig. 8) indicated that piperine (C-4), methylpiperate (C-2), and piperlongumine (C-5) remained in the yellow zone. The log Kp value predicted that the test molecules

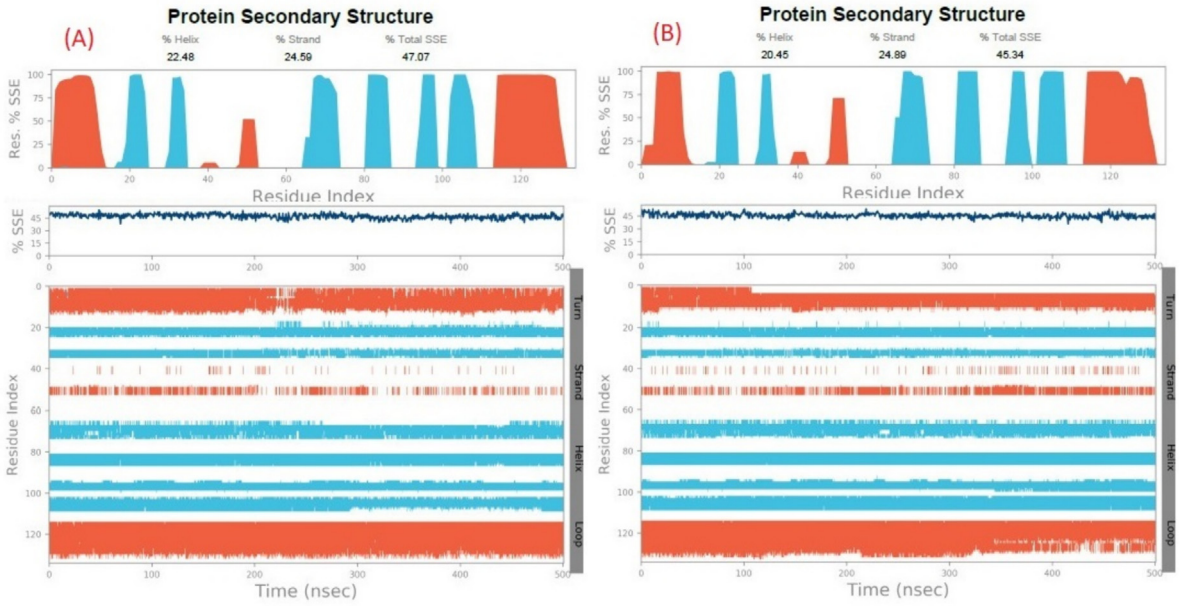

Fig. 7. Secondary structure analysis of A42R profilin-like protein in complex with (A) kaempferol (C-1) and (B) piperine (C-4).

Table 3
QSAR assessment of optimised compounds.

Physical characteristics	C-1: Kaempferol	C-2: Methyl piperate	C-3: Myricetin	C-4: Piperine	C-5: Piperlongumine	C-6: Quercetin
Surface area (Approx) (Å^2)	380.91	456.02	398.27	489.68	559.20	388.23
Surface area (Grid) (Å^2)	478.79	475.53	493.66	454.22	591.46	485.96
Volume (Å^3)	774.17	739.99	810.06	904.65	971.48	791.18
Hydration energy (kcal/mole)	−29.69	−10.73	−41.04	−6.87	−7.89	−35.68
Log P	4.40	4.39	4.05	5.25	5.92	4.22
Refractivity (Å^3)	18.04	22.99	20.81	42.11	43.57	19.22
Polarisability (Å^3)	27.90	24.12	29.18	31.40	32.89	28.54
Mass (amu)	286.24	232.24	318.24	285.34	317.34	302.24
Total energy (kcal/mol)	8.78886	16.3107	9.44994	23.9282	13.9124	9.71479
Dipole moment (Debye)	1.638	0.2963	3.456	0.5324	0.3267	2.482
Free energy (kcal/mol)	8.78886	16.3107	9.44994	23.9282	13.9124	9.71479
RMS gradient (kcal/ Å mol)	0.09854	0.09275	0.09028	0.0965	0.09399	0.08983

had low skin permeation (Table 4) but passively permeated the BBB (Fig. 8).

Table 5 lists the drug-like behavior of the test phytocompounds (C-1 to C-6). All compounds, except myricetin (C-3), possessed zero Lipinski, Ghose, Veber and Egan violations. BBB crossing, as an important parameter, was explained by the topological polar surface area (TPSA) value that ranged between 20 and 130 Å^2.[56] The values were within an acceptable range for all compounds except myricetin (C-3) and quercetin (C-6), with piperine (C-4) returning the lowest (38.77 Å^2) value (Table 5). The Consensus log P value was within the permissive limit of <6 for all compounds.

In silico toxicity assessment of the compounds using the pkSCM server indicated no compound was toxic (Table 6). The AMES values of kaempferol and piperine were negative, indicating that both were non-mutagenic. Additionally, neither compound was an hERG I/II inhibitor, indicating that the molecules prohibited long QT syndrome, which led to cardiac signaling disorder. The LD_{50} values of the compounds were comparable. There was a difference in the LOAEL values. Piperine had a LOAEL value of 1.742, and the value for kaempferol was 2.505. Although piperine showed a hepatotoxicity trait, it was established that a calculated restricted amount was permissible. Based on the toxicity, piperine was a slightly more suitable drug candidate than kaempferol. Overall, data analysis showed that piperine (C-4) is a potential candidate for treating mpox, with further validation of the findings required.

Table 4
ADME properties of the compounds.

Compound	GI absorption	BBB permeantion	Pgp substrate	CYP1A2 inhibitor	CYP2C19 inhibitor	CYP2C9 inhibitor	CYP2D6 inhibitor	CYP3A4 inhibitor	log Kp (cm/s)
Kaempferol (C-1)	High	No	No	Yes	No	No	Yes	Yes	−6.7
Methyl piperate (C-2)	High	Yes	No	Yes	Yes	Yes	No	No	−5.9
Myricetin (C-3)	Low	No	No	Yes	No	No	No	Yes	−7.4
Piperine (C-4)	High	Yes	No	Yes	Yes	Yes	No	No	−5.58
Piperlongumine (C-5)	High	Yes	No	No	No	No	No	No	−6.77
Quercetin (C-6)	High	No	No	Yes	No	No	Yes	Yes	−7.05

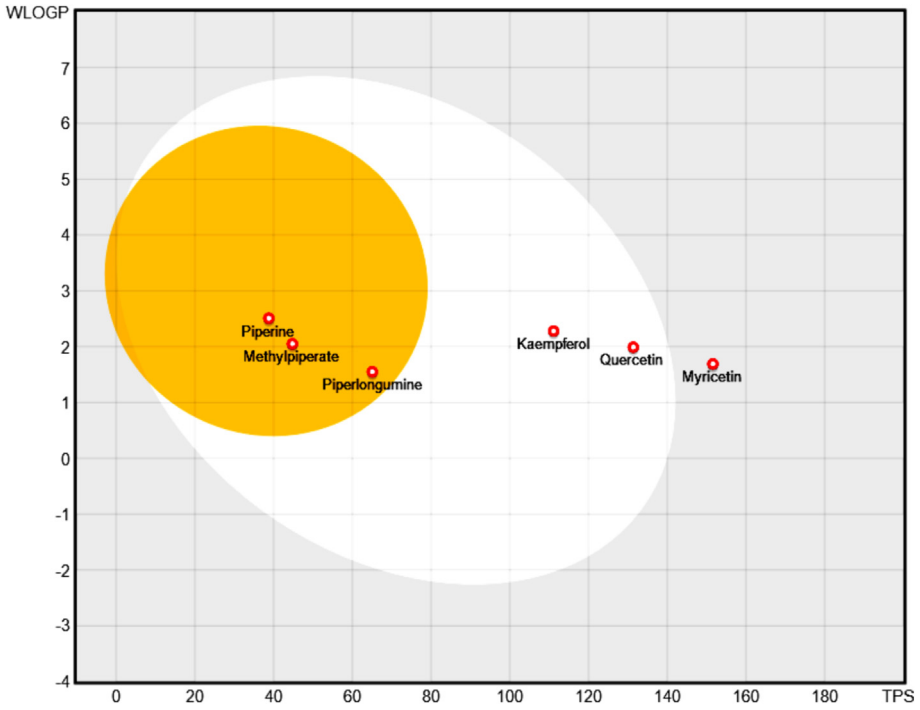

Fig. 8. Generated boiled egg graph for (C-1–C-6) test phytocompounds as drug candidates.

Table 5
Drug-likeness properties of the compounds.

Compound	MW (g/mol)	Rotatable bonds	H-bond acceptors	H-bond donors	TPSA (Å^2)	Consensus Log P	Lipinski violations	Ghose violations	Veber violations	Egan violations	Muegge violations	Bioavailability Score	Synthetic Accessibility
Kaempferol (C-1)	286.24	1	6	4	111.13	1.58	0	0	0	0	0	0.55	3.14
Methyl piperate (C-2)	232.23	4	4	0	44.76	2.62	0	0	0	0	0	0.55	2.89
Myricetin (C-3)	318.24	1	8	6	151.59	0.79	1	0	1	1	2	0.55	3.27
Piperine (C-4)	285.34	4	3	0	38.77	3.03	0	0	0	0	0	0.55	3.23
Piperlongumine (C-5)	317.34	6	5	0	65.07	1.96	0	0	0	0	0	0.55	3.18
Quercetin (C-6)	302.24	1	7	5	131.36	1.23	0	0	0	0	0	0.55	3.23

Table 6
Toxicity data of the six selected phytocompounds.

Compound	AMES toxicity	Max. tolerated dose (human)	hERG I inhibitor	hERG II inhibitor	Oral Rat Acute Toxicity (LD_{50})	Oral Rat Chronic Toxicity (LOAEL)	Hepato-toxicity	Skin sensitivity	*T. pyriformis* toxicity	Minnow toxicity
Kaempferol (C-1)	No	0.531	No	No	2.449	2.505	No	No	0.312	2.885
Methyl piperate (C-2)	No	0.494	No	No	2.073	1.673	No	No	1.349	0.46
Myricetin (C-3)	No	0.822	No	No	2.784	2.775	No	No	0.287	2.717
Piperine (C-4)	No	−0.516	No	No	2.493	1.754	Yes	No	1.931	1.202
Piperlongumine (C-5)	No	0.451	No	No	2.424	1.538	No	No	1.055	1.415
Quercetin (C-6)	No	0.775	No	No	2.607	2.464	No	No	0.335	1.957

4. Limitations and challenges

This study considered only one mpox protein (which was analyzed in greater detail) and ascertained the interaction of this protein with several compounds. Further studies can extend to other mpox proteins. The vaccine and drug efficacies of the identified mpox protein are unknown, which is required. Furthermore, the drug effect by combining the two (C-1 and C-4) promising phytocompounds should be examined rather than confirming a single selected phytochemical as a drug candidate, which is in line with other combinatorial medicines. Mpox has been declared a neglected tropical disease, which shows that the global research and development interest in mpox has remained limited. This issue has resulted in inadequate knowledge of the various critical aspects of the etiology and the etiological agent of its occurrence and the associated human health concerns.

This reported work is essentially a computational study. Hence, the findings need to be further confirmed and validated by addi-

tional dry-laboratory (e.g., PCA) and wet-laboratory (*in vitro* and *in vivo*) research, and clinical trials can then be conducted. This effort should provide efficacy on the selected compounds (C-1 and C-4). Further, international cooperation in a concerted effort to find workable global solutions is needed and highly recommended.

5. Conclusions

There is growing interest in using phytocompounds to combat viral infections. Interaction studies against A42R profilin-like protein from mpox and ADMET of six phytochemicals identified C-1 (kaempferol) and C-4 (piperine) as lead candidates. Piperine (C-4) with a predicted IC_{50} of 7.63 μM displayed the strongest binding (–6.98 kcal/mol) energy, as determined by docking analysis. The binding energy for kaempferol (C-1) was –5.57 kcal/mol with a significant ADMET. MD simulations revealed that C-1 and C-4 formed stable P-L complexes with the target protein. As per P-L interactions, kaempferol (C-1) exhibited all (water bridges, hydrophobic, ionic and H-bonding) non-covalent interactions. The Log P values of the compounds were appreciable and between 4 and 6, the highest being for piperlongumine (5.92) and piperine (5.25). The lowest TPSA toxicity value (38.77 $Å^2$) was found for piperine (C-4). Pharmacokinetics, drug-likeness and QSAR results indicated that C-4 and C-1 are potential lead candidates to validate, design and develop novel drugs against mpox. The negative AMES values of C-1 and C-4 indicated that both were non-mutagenic. C-4 showed slightly lower toxicity compared with C-1. A comprehensive study to confirm and validate the potential of the phytocompounds to treat mpox is recommended. These compounds can be recommended for drug design after *in vitro* validation and *in vivo* authentication. Analysis of other promising phytochemicals using cutting-edge technologies should offer a range of new innovative therapeutics for untreatable etiological pathogeneses.

Declarations

All authors have read the manuscript, participated in revisions, and approved the publication of the work.

Funding

No funding was received.

CRediT authorship contribution statement

Ranjan K. Mohapatra: Conceptualization, Supervision, Writing – original draft. **Ahmed Mahal:** Data curation, Writing – original draft. **Pranab K. Mohapatra:** Formal analysis, Methodology, Writing – original draft. **Ashish K. Sarangi:** Formal analysis, Methodology, Writing – original draft. **Snehasish Mishra:** Project administration, Writing – review & editing. **Meshari A. Alsuwat:** Validation, Writing – original draft. **Nada N. Alshehri:** Validation, Writing – original draft. **Sozan M. Abdelkhalig:** Validation, Writing – original draft. **Mohammed Garout:** Validation, Writing – original draft. **Mohammed Aljeldah:** Data curation, Writing – original draft. **Ahmad A. Alshehri:** Data curation, Writing – original draft. **Ahmed Saif:** Data curation, Writing – original draft. **Mohammed Abdulrahman Alshahrani:** Data curation, Writing – original draft. **Ali S. Alqahtani:** Validation, Writing – original draft. **Yahya A. Almutawif:** Validation, Writing – original draft. **Hamza M. Ali:** Validation, Writing – original draft. **Faisal M Albaqami:** Validation, Writing – original draft. **Mohnad Abdalla:** Formal analysis, Methodology, Writing – original draft. **Ali A. Rabaan:** Project administration, Writing – review & editing.

Declaration of competing interest

The authors declare that they have no known competing financial interests or personal relationships that could have appeared to influence the work reported in this paper.

Acknowledgments

RKM and PKM acknowledge Prof. Mukesh K. Raval for sharing his expertise. All authors thank their respective institutions/affiliations for the necessary support received.

References

1. Mohapatra RK, Tuli HS, Sarangi AK, et al. Unexpected sudden rise of human monkeypox cases in multiple non-endemic countries amid COVID-19 pandemic and salient counteracting strategies: Another potential global threat? *Int J Surg*. 2022;103:106705.
2. WHO. Disease outbreak news; multi-country monkeypox outbreak in non-endemic countries. World Health Organization; 2022. https://www.who.int/emergencies/disease-outbreak-news/item/2022-DON385 (accessed on July 19, 2022).
3. WHO. WHO Director-General declares the ongoing monkeypox outbreak a Public Health Emergency of International Concern; 23 July 2022. https://www.who.int/europe/news/item/23-07-2022-who-director-general-declares-the-ongoing-monkeypox-outbreak-a-public-health-event-of-international-concern#:~:text=On%20July%2023%2C%20the%20WHO,of%20International%20Concern%20(PHEIC) (accessed on 15-11-22).
4. Bunge EM, Hoet B, Chen L, et al. The changing epidemiology of human monkeypox—A potential threat? A systematic review. *PLOS Negl Trop Dis*. 2022;16(2):e0010141.
5. WHO. Multi-country outbreak of monkeypox; 2022. https://cdn.who.int/media/docs/default-source/2021-dha-docs/20220706_monkeypox_external_sitrep_final.pdf?sfvrsn=1b580b3d_4&download=true (accessed on July 19, 2022).
6. Yadav PD, Reghukumar A, Sahay RR, et al. First two cases of Monkeypox virus infection in travellers returned from UAE to India, July 2022. *J Infect*. 2022;85(5):E145–E148. https://doi.org/10.1016/j.jinf.2022.08.007.
7. Orviz E, Negredo A, Ayerdi O, et al. Monkeypox outbreak in Madrid (Spain): clinical and virological aspects. *J Infect*. 2022;85(4):412–417. https://doi.org/10.1016/j.jinf.2022.07.005.
8. Thornhill JP, Barkati S, Walmsley S, et al. Monkeypox virus infection in humans across 16 countries - April–June 2022. *N Engl J Med*. 2022;387:679–691. https://doi.org/10.1056/nejmoa2207323.
9. Raccagni AR, Mileto D, Canetti D, et al. Monkeypox and pan-resistant Campylobacter spp infection in Entamoeba histolytica and Chlamydia trachomatis re-infection in a man who have sex with men. *J Infect*. 2022;85(4):436–480. https://doi.org/10.1016/j.jinf.2022.06.028.
10. Ahmed SK, Mohamed MG, Dabou EA, et al. Monkeypox (mpox) in immunosuppressed patients. *F1000Research*. 2023;12:127.
11. Shuvo PA, Roy A, Dhawan M, et al. Recent outbreak of monkeypox: Overview of signs, symptoms, preventive measures, and guideline for supportive management. *Int J Surg*. 2022;105:106877.
12. Nolasco S, Vitale F, Geremia A, et al. First case of monkeypox virus, SARS-CoV-2 and HIV co-infection. *J Infect*. 2022;86(1):E21–E23. https://doi.org/10.1016/j.jinf.2022.08.014.
13. Chandran D, Hridya P, Prasanth D, et al. Changing patterns in the spread of human monkeypox: A dangerous new development in disease epidemiology. *J Pure Appl Microbiol*. 2022;16(suppl 1):3106–3118.
14. Rizk JG, Lippi G, Henry BM, et al. Prevention and Treatment of Monkeypox. *Drugs*. 2022;82(9):957–963. https://doi.org/10.1007/s40265-022-01742-y.
15. Chopra H, Dhawan M, Bibi S, et al. FDA approved vaccines for monkeypox: Current eminence. *Int J Surg*. 2022;105:106896.
16. Diaz JH. The disease ecology, epidemiology, clinical manifestations, management, prevention, and control of increasing human infections with animal orthopoxviruses. *Wilderness Environ Med*. 2021;32(4):528–536. https://doi.org/10.1016/j.wem.2021.08.003.
17. Rodríguez-Cuadrado FJ, Pinto-Pulido EL, Fernández-Parrado M. RF-Potential treatments for monkeypox. *Actas Dermosifiliogr*. 2022;114(7):629–630. https://doi.org/10.1016/j.ad.2022.06.013.
18. Sethi Y, Agarwal P, Murli H, et al. Neuropsychiatric manifestations of monkeypox: A clinically oriented comprehensive review. *Brain and Behavior*. 2023;13:e2934.
19. Mohapatra RK, Mishra S, Rabaan AA, et al. Monkeypox breakthrough infections and side-effects: Clarion call for nex-gen novel vaccine. *New Microbes New Infect*. 2023;52:101084.
20. Sahu R, Mohapatra RK, Al-Resayes SI, et al. An efficient synthesis towards the core of Crinipellin: TD-DFT and docking studies. *J Saudi Chem Soc*. 2021;25:101193.
21. Mohapatra RK, Dhama K, El-Arabey AA, et al. Repurposing benzimidazole and benzothiazole derivatives as potential inhibitors of SARS-CoV-2: DFT, QSAR,

molecular docking, molecular dynamics simulation, and in-silico pharmacokinetic and toxicity studies. *J King Saud Univ – Sci*. 2021;33:101637.
22. Mohapatra RK, Azam M, Mohapatra PK, et al. Computational studies on potential new anti-Covid-19 agents with a multi-target mode of action. *J King Saud Univ – Sci*. 2022;34:102086.
23. Abdalla M, Mohapatra RK, Sarangi AK, et al. In silico studies on phytochemicals to combat the emerging COVID-19 infection. *J Saudi Chem Soc*. 2021;25:101367. https://doi.org/10.1016/j.jscs.2021.101367.
24. Ghate SD, Pinto L, Alva S, et al. In silico identification of potential phytochemical inhibitors for mpox virus: molecular docking, MD simulation, and ADMET studies. *Mol Divers*. 2024. https://doi.org/10.1007/s11030-023-10797-2.
25. Akash S, Mir SA, Mahmood S, et al. Novel computational and drug design strategies for inhibition of monkeypox virus and Babesia microti: molecular docking, molecular dynamic simulation and drug design approach by natural compounds. *Front Microbiol*. 2023;14:1206816. https://doi.org/10.3389/fmicb.2023.1206816.
26. Vardhan S, Sahoo SK. Computational studies on searching potential phytochemicals against DNA polymerase activity of the monkeypox virus. *J Tradit Complement Med*. 2023;13:465–478.
27. Dutt M, Kumar A, Rout M, et al. Drug repurposing for Mpox: Discovery of small molecules as potential inhibitors against DNA-dependent RNA polymerase using molecular modeling approach. *J Cell Biochem*. 2023;124:701–715.
28. Sahoo AK, Augusthian PD, Muralitharan I, et al. In silico identifcation of potential inhibitors of vital monkeypox virus proteins from FDA approved drugs. *Mol Divers*. 2023;27:2169–2184.
29. Patel CN, Mall R, Bensmail H. AI-driven drug repurposing and binding pose meta dynamics identifies novel targets for monkeypox virus. *J Infect Public Health*. 2023;16:799–807.
30. Bansal P, Gupta M, Sangwan S, et al. Computational purposing phytochemicals against cysteine protease of monkeypox virus: An in-silico approach. *J Pure Appl Microbiol*. 2022;16(suppl 1):3144–3154.
31. Gulati P, Chadha J, Harjai K, Singh S. Targeting envelope proteins of poxviruses to repurpose phytochemicals against monkeypox: An in silico investigation. *Front Microbiol*. 2023;13:1073419. https://doi.org/10.3389/fmicb.2022.1073419.
32. Patel M, Bazaid A. Novel phytochemical inhibitors targeting monkeypox virus thymidine and serine/threonine kinase: integrating computational modelling and molecular dynamics simulation. *J Biomol Struct Dyn*. 2023;41(6):1–17. https://doi.org/10.1080/07391102.2023.2179547.
33. Imran M, Abida ANM, et al. Repurposing anti-dengue compounds against monkeypox virus targeting core cysteine protease. *Biomedicines*. 2023;11:2025. https://doi.org/10.3390/biomedicines11072025.
34. Minasov G, Inniss NL, Shuvalova L, et al. Structure of the Monkeypox virus profilin-like protein A42R reveals potential functional differences from cellular profilins. *Acta Crystallogr F Struct Biol Commun*. 2022;78:371–377.
35. Mohapatra RK, Mahal A, Ansari A, et al. Comparison of the binding energies of approved mpox drugs and phytochemicals through molecular docking, molecular dynamics simulation, and ADMET studies: An in silico approach. *J Biosaf Biosecurity*. 2023;5:118–132.
36. Dassanayake MK, Khoo T-J, Chong CH, et al. Molecular docking and in-silico analysis of natural biomolecules against Dengue, Ebola, Zika, SARS-CoV-2 variants of concern and Monkeypox Virus. *Int J Mol Sci*. 2022;23:11131.
37. Banik A, Ahmed SR, Shahid SB, et al. Therapeutic promises of plant metabolites against monkeypox virus: An in silico study. *Adv Virol*. 2023:9919776. https://doi.org/10.1155/2023/9919776.
38. Chandrasekar SB, Bhanumathy M, Pawar AT, Somasundaram T. Phytopharmacology of Ficus religiosa. *Phcog Rev*. 2010;4(8):195–199.
39. Murugesu S, Selamat J, Perumal V. Phytochemistry, pharmacological properties, and recent applications of Ficus benghalensis and Ficus religiosa. *Plants*. 2021;10:2749. https://doi.org/10.3390/plants10122749.
40. Krieger E, Joo K, Lee J, et al. Improving physical realism, stereochemistry, and side-chain accuracy in homology modeling: Four approaches that performed well in CASP8. *Proteins*. 2009;77:114–122.
41. Mohapatra RK, Saikishore VP, Azam M, Biswal SK. Synthesis and physicochemical studies of a series of mixedligand transition metal complexes and their molecular docking investigations against Coronavirus main protease. *Open Chem*. 2020;18:1495–1506.
42. Al-Noor TH, Mohapatra RK, Azam M, et al. Mixed-ligand complexes of ampicillin derived Schiff base ligand and Nicotinamide: Synthesis, physico-chemical studies, DFT calculation, antibacterial study and molecular docking analysis. *J Mol Struct*. 2021;1229:129832.
43. Mohapatra RK, El-ajaily MM, Alassbaly FS, et al. DFT, anticancer, antioxidant and molecular docking investigations of some ternary Ni(II) complexes with 2-[(E)-[4-(dimethylamino)phenyl]methyleneamino]phenol. *Chem Pap*. 2021;75:1005–1019.
44. Schrodinger Release 2020-1. Glide, phase, ligprep. Schrodinger, LLC; 2020.
45. Daina A, Michielin O, Zoete V. SwissADME: a free web tool to evaluate pharmacokinetics, drug-likeness and medicinal chemistry friendliness of small molecules. *Sci Rep*. 2017;7:42717.
46. Pires DE, Blundell TL, Ascher DB. pkCSM: predicting small-molecule pharmacokinetic and toxicity properties using graph-based signatures. *J Med Chem*. 2015;58(9):4066–4072.
47. Morris GM, Huey R, Lindstrom W, et al. AutoDock4 and AutoDockTools4: automated docking with selective receptor flexibility. *J Comput Chem*. 2009;30(16):2785–2791.
48. Morris GM, Goodsell DS, Halliday RS, et al. Automated docking using a Lamarckian genetic algorithm and an empirical binding free energy function. *J Comput Chem*. 1998;19:1639–1662.
49. Al M, Kumer A, Mukerjee N, et al. Mechanistic inhibition of Monkeypox and Marburg virus infection by O-rhamnosides and Kaempferol-o-rhamnosides derivatives: a new-fangled computational approach. *Front Cell Infect Microbiol*. 2023;13:1188763. https://doi.org/10.3389/fcimb.2023.1188763.
50. Pant S, Singh M, Ravichandiran V, et al. Peptidelike and small-molecule inhibitors against Covid-19. *J Biomol Struct Dyn*. 2020;39(8):2904–2913.
51. Shivanika C, Kumar SD, Ragunathan V, et al. Molecular docking, validation, dynamics simulations, and pharmacokinetic prediction of natural compounds against the SARS-CoV-2 main-protease. *J Biomol Struct Dyn*. 2020;40(2):585–611. https://doi.org/10.1080/07391102.2020.1815584.
52. Beura S, Chetti P. In-silico strategies for probing chloroquine based inhibitors against SARS-CoV-2. *J Bimol Struct Dyn*. 2021;39(10):3747–3759. https://doi.org/10.1080/07391102.2020.1772111.
53. Kumar S, Sharma PP, Shankar U, et al. Discovery of new hydroxyethylamine analogs against 3CLpro protein target of SARS-CoV-2: Molecular docking, molecular dynamics simulation, and structure–activity relationship studies. *J Chem Inf Model*. 2020;60:5754–5770.
54. Dariya B, Nagaraju GP. Understanding novel COVID-19: Its impact on organ failure and risk assessment for diabetic and cancer patients. *Cytokine Growth Factor Rev*. 2020;53:43–52. https://doi.org/10.1016/j.cytogfr.2020.05.001.
55. Padmanabhan J, Parthasarathi R, Subramanian V, Chattaraj P. Electrophilicity-based charge-transfer descriptor. *J Phys Chem*. 2007;111:1358–1361. https://doi.org/10.1021/jp0649549.
56. Ertl P, Rohde B, Selzer P. Fast calculation of molecular polar surface area as a sum of fragment-based contributions and its application to the prediction of drug transport properties. *J Med Chem*. 2000;43(20):3714–3717.